Received: 17 March 2020 | Revised: 12 August 2020 | Accepted: 2 September 2020

DOI: 10.1002/jmor.21269

RESEARCH ARTICLE

morphology WILEY

Comparative morphology of shark pectoral fins

Sarah L. Hoffmann[1] | Thaddaeus J. Buser[2] | Marianne E. Porter[3]

[1]Applied Biological Services, Biomark, Inc., Boise, Idaho

[2]Department of Fisheries and Wildlife, Oregon State University, Corvallis, Oregon

[3]Department of Biological Sciences, Florida Atlantic University, Boca Raton, Florida

Correspondence
Sarah L. Hoffmann, Applied Biological Services, Biomark, Inc., Boise, ID.
Email: slhoffmann2014@gmail.com

Funding information
Florida Atlantic University; Florida Atlantic University Newell Doctoral Fellowship; Delores. A. Auzenne Fellowship

Abstract

Sharks vary greatly in morphology, physiology, and ecology. Differences in whole body shape, swimming style, and physiological parameters have previously been linked to varied habitat uses. Pectoral fin morphology has been used to taxonomically classify species and hypotheses on the functional differences in shape are noted throughout the literature; however, there are limited comparative datasets that quantify external and skeletal morphology. Further, fins were previously categorized into two discrete groups based on the amount of skeletal support present: (a) aplesodic, where less than half of the fin is supported and (b) plesodic where greater than half of the fin is supported. These discrete classifications have been used to phylogenetically place species, though the methodology of classification is infrequently described. In this study, we sampled fins from 18 species, 6 families, and 3 orders, which were also grouped into five ecomorphotype classifications. We examined the external morphology, extent of skeletal support, and cross-sectional shape of individual cartilaginous elements. Using phylogenetic comparative methods, we show that fin shape does not differ significantly between ecomorphotypes, suggesting there may be some mechanical constraint. However, we find that the internal anatomy of the fin does vary significantly between ecomorphotypes, especially the extent and distribution of calcification of skeletal support, suggesting that the superficial similarity of fin shapes across ecomorphotypes may belie differences in function. Finally, we find that a number of morphological variables such as number of radials, radial calcification and shape, and fin taper all correlate with the extent of skeletal support. Within these morphospaces, we also describe that some orders/families tend to occupy certain areas with limited overlap. While we demonstrate that there is some mechanical constraint limiting external variations in shark pectoral fin morphology, there are compounding differences in skeletal anatomy that occur within ecomorphotypes which we propose may affect function.

KEYWORDS

ecomorphology, elasmobranch, phylogenetic comparative methods

1 | INTRODUCTION

Control surfaces, or structures that manipulate an organism's position in space, vary greatly in morphology among aquatic vertebrates (Fish & Lauder, 2017; Lucas, Lauder, & Tytell, 2020). For many open ocean swimmers (some marine mammals, sea turtles, oceanic fishes), control surfaces are shaped like hydrofoils (thicker leading edges that taper posteriorly) which tend to be less flexible to promote lift generation (Fish & Lauder, 2017). Aquatic vertebrates that are associated with more architecturally complex environments (reef associated

fishes) have more flexible fins that may be used for increased maneuverability (Blake, 2004; Lauder & Drucker, 2004). In contrast, long, stiff fins are likely less maneuverable and may not be ideal for animals swimming in complex environments. External fin shape is also shown to change among habitat use where open ocean species have long, thin fins and benthic associated species have shorter, wider fins (Fish & Lauder, 2017; Fulton, Bellwood, & Wainwright, 2005; Wainwright, Bellwood, & Westneat, 2002). These comparisons are often made using aspect ratio (AR), the ratio of fin length to area, which affects the amount of lift produced relative to drag (Vogel, 1994; Webb, 1975; Weber, Howe, Murray, Reidenberg, & Fish, 2014; Weber, Howle, Murray, & Fish, 2009).

As is demonstrated in other fishes, it is hypothesized that variations in shark pectoral fin morphology may reflect ecological differences (Maia, Wilga, & Lauder, 2012; Sakai, 2011). There are also varied descriptions of shark pectoral fin function that may be the result of different study species (Daniel, 1922; Fish & Shannahan, 2000; Harris, 1936; Wilga & Lauder, 2000, 2001). Historically, shark pectoral fins are hypothesized to generate lift that balances the body during steady swimming (Daniel, 1922; Ferry & Lauder, 1996; Fish & Shannahan, 2000; Harris, 1936). For at least one benthic shark species, negligible lift is generated by the pectoral fins during steady swimming and the anterior body generates the balancing lift force (Wilga & Lauder, 2000). In general, our understanding of the comparative morphology of sharks is limited to species that are easy to access and/or are successful in captivity, making an ecomorphological assessment of pectoral fins challenging.

In addition to external variations in morphology, shark pectoral fin skeleton is also documented to vary among species. In general, three basal elements (propterygium, mesopterygium, and metapterygium) articulate with the scapulocoracoid at the proximal fin base (Figure 1; Liem & Summers, 1999; Marinelli & Strenger, 1959). Three series of radial elements extend distally into the fin web from the basals (Figure 1; Marinelli & Strenger, 1959; Liem & Summers, 1999). Thin, flexible ceratotrichia are embedded in the dense connective tissue that anchors the skeleton to the fin (Marinelli & Strenger, 1959; Liem & Summers, 1999). Differences in the relative amount of radial support in the fin (concentrated in the proximal fin region) have been described throughout the literature as a diagnostic characteristic that was historically used in phylogenetic classification (Compagno, 1977; Compango, 1990; Maisey, 1984; Shirai, 1996). Fins with less than 50% radial support are considered aplesodic while fins with greater than 50% radial support are plesodic (Compagno, 1977; Maia et al., 2012). These classifications vary within families and orders, though the method of classification is often undescribed and may not be comparable among all studies (Figure 2; Bendix-Almgreen, 1975; Compagno, 1973, 1977, 1988; Zangerl, 1973; Maisey, 1984; Maia et al., 2012; Crawford, 2014).

Differences in the extent of skeletal support in the fin, hereafter skeletal extent, would likely affect the mechanical behavior of the fin. Fins with more skeletal support may be stiffer, and thus, more efficient as hydrofoils; whereas flexible fins may be better suited for maneuverability (Maia et al., 2012). An inverse relationship between skeletal extent and muscle mass has been described among a few species, further suggesting that there may be a finer degree of control over flexible, maneuverable fins (Maia et al., 2012). Obtaining samples from a broad spectrum of species and ecomorphotypes (which we define as groups of species with similar morphological and ecological traits [Table 1]) is likely a factor in the lack of a comprehensive comparative dataset. Throughout the literature, studies hypothesize that there is an ecomorphological trend in fin morphology without being able to make direct comparison. Thus, our goal was to evaluate a variety of morphological characteristics from as broad a sample as we

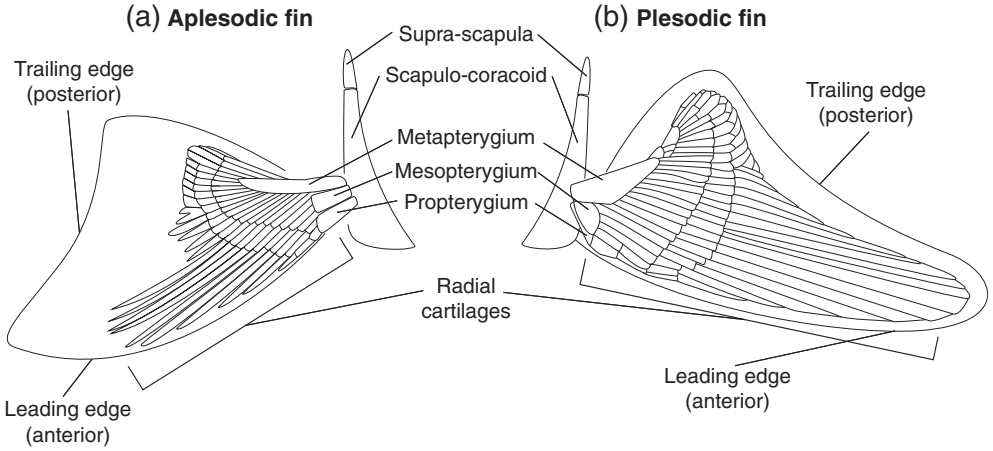

FIGURE 1 Gross anatomy of cartilaginous skeletal elements in shark pectoral fins. Fins generally have a longer, tapered leading edge (anterior) and a trailing edge (posterior) fork that terminates in a lobe. Internally, three basal cartilages (the propterygium, mesopterygium, and metapterygium) articulate at the proximal fin base with the scapulo-coracoid. Three sets of radials (proximal, intermediate, and distal) extend distally from the basals to support the fin web. Thin, flexible ceratotrichia are embedded in the connective tissue that overlays the skeleton and attaches it to the fin. Fins have been categorized based on the extent to which the skeletal elements (radials) extend into the fin web. If less than 50% of the fin web is supported by the skeletal elements, the fin is termed "aplesodic" (a), whereas greater than 50% skeletal support is considered "plesodic" (b). For both fin types, the leading edge lobe is generally more supported by the radials, and thus more rigid, than the trailing edge lobe

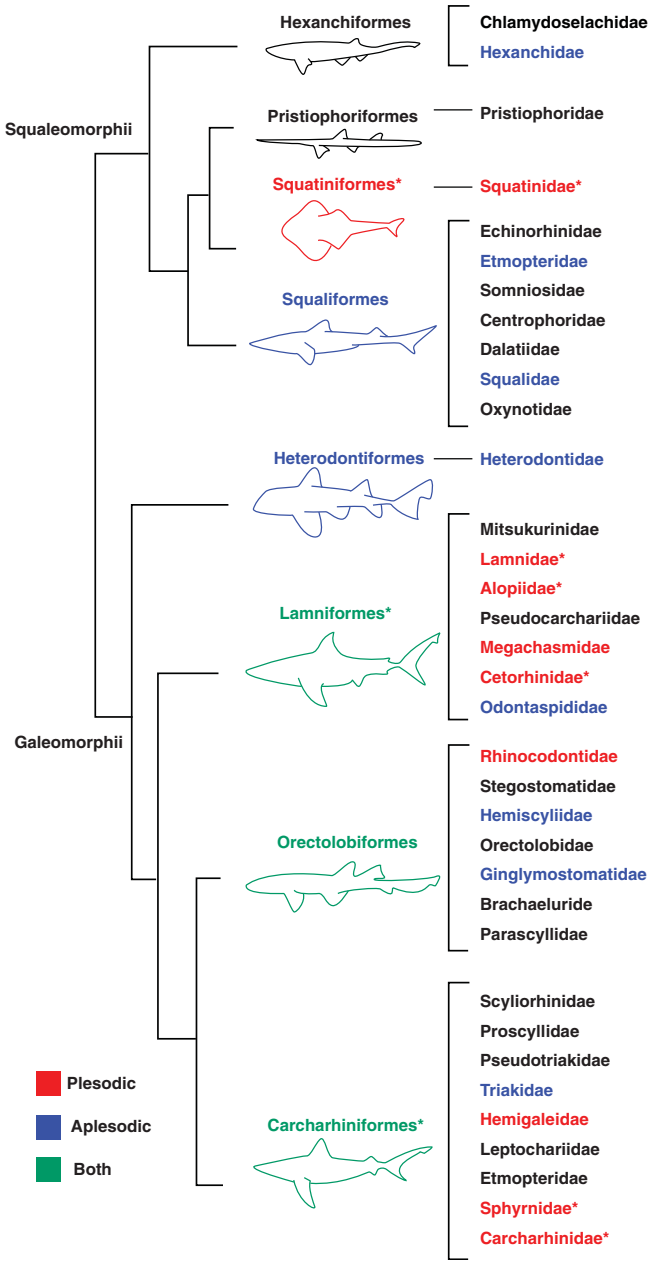

FIGURE 2 Shark fin classification by family (Phylogeny: Velez-Zuazo & Agnarsson, 2011; Classifications: Compagno, 1977; Maisey, 1984; Wilga & Lauder, 2001; Maia et al., 2012; Sakai, 2011; Crawford, 2014). Colors represent prior fin classifications and the families represented in this study are starred

could collect. Notably, this paper is also challenged by access to specimens, especially considering the protected and endangered status of some species represented, leading to uneven and limited sample sizes. We present these data with suggestions for future sampling efforts.

Based on trends from the literature, we hypothesized that there would be an ecomorphological gradient in fin morphology from benthic to oceanic species (Sakai, 2011; Maia et al., 2012). We predicted that at one end of the spectrum, oceanic species would have high AR fins with extensive skeletal support that maximize hydrodynamic efficiency, whereas benthic species would have low AR fins with limited skeletal support for increased flexibility and maneuverability, with other ecomorphotypes falling in order of their body size, habitat use, and migratory behavior. Similarly, we predicted that the skeletal elements of oceanic species would be highly calcified and laterally compressed, while benthic species would have dorsoventrally compressed radials with limited calcification. We also hypothesized that the cross-sectional variables we measured would correlate to skeletal extent and AR such that benthic species (Ecomorphotype A) have the least skeletal support, smallest AR, most dorso-ventrally compressed radials, and least radial calcification, while the opposite for each would be true on the oceanic end of the spectrum (Ecomorphotypes D and E). To address this, we assess the external and skeletal morphology of pectoral fins from 18 species (six families, three orders) among five ecomorphotype classifications and families. We measured a variety of morphological features and used phylogenetic comparative methods to test our ecomorphological hypotheses in phylogenetic context. We also examined relationships among measured variables to evaluate patterns in morphology observed among all species in the study.

2 | METHODS

2.1 | Material collection

Fins were examined from 18 species: six families, three orders (Table 1). Shark pectoral fins were opportunistically sampled from various strandings, at vessel mortalities, fishing tournaments, and donated from various researchers from species in the Western Atlantic (National Marine Fisheries Service Exempt Fishing Permit Highly Migratory Species Management Division SHK-EFP-19-02, 6 April 2017). All fins were fresh frozen upon sampling and thawed completely before dissection. Due to the numerous methods and people used to obtain fins, there was variability in the way fins were removed from the trunk. We standardized the fin "base" as a perpendicular line from leading edge to the posterior end of the curvature of the trailing edge lobe (Figure 3a). The data presented here represent the radial cartilages and do not include the most proximal portion of the pectoral fin including the three basal cartilages that articulate with the scapula-coracoid at the proximal body axis (Liem & Summers, 1999; Maia et al., 2012; Marinelli & Strenger, 1959). Additionally, we were not able to collect size and life stage information for all samples, which are factors that cannot be captured in our results.

Species were grouped into five ecomorphotypes to examine morphology in an ecological context (Table 1; Compagno, 1984). Ecomorphotypes were categorized based on habitat use, average body size at maturity, and migratory behavior. Ecomorphotype A represented the only benthic species in this study, the Atlantic angel shark, which frequently interacts with the seafloor, sometimes burying in the substrate. This was also the only species in the study that was not an obligate ram ventilator. Ecomorphotype E was also only represented by one species, the basking shark, which was the largest species in this study and the only filter feeder. Individuals of this species are generally slow swimmers that migrate through temperate waters, often close to shore.

TABLE 1 Sample size, habitat use, and migratory behavior of species encompassed in the present study (Compagno, 1984). These variables were used to categorize species into five ecomorphotypes: (A) benthic, obligate-ram ventilating species known to rest on the seafloor for long periods of time; (B) small bodied, nonmigratory species; (C) medium sized, migratory species; (D) large bodied, migratory species, and (E) largest, filter feeding migratory species

n		Habitat	Migratory?	Size at maturity (cm)	Ecomorphotype
Squatiniformes					
	Squatinidae				
4	*Squatina dumeril*	Bathydemersal	N	92–107	A
Carcharhiniformes					
	Carcharhinidae				
1	*Carcharhinus acronotus*	Reef associated	N	103–137	B
8	*Rhizoprionodon terraenovae*	Demersal	N	85–90	B
6	*Carcharhinus limbatus*	Reef associated	Y	120–194	C
1	*Carcharhinus isodon*	Demersal	Y	150–139	C
2	*Carcharhinus plumbeus*	Benthopelagic	Y	126–183	C
2	*Prionace glauca*	Oceanic-epipelagic	Y	173–281	D
4	*Carcharhinus obscurus*	Coastal-pelagic	Y	220–300	D
2	*Carcharhinus falciformis*	Oceanic-epipelagic	Y	202–260	D
1	*Galeocerdo cuvier*	Benthopelagic	Y	210–350	D
	Sphyrnidae				
5	*Sphyrna tiburo*	Reef associated	N	80–90	B
3	*Sphyrna lewini*	Coastal-pelagic	Y	140–273	C
2	*Sphyrna mokarran*	Coastal-pelagic	Y	210–300	D
Lamniformes					
	Lamnidae				
5	*Lamna nasus*	Oceanic	Y	170–180	D
4	*Carcharodon carcharias*	Oceanic	Y	450–500	D
4	*Isurus oxyrinchus*	Oceanic	Y	275–285	D
	Alopiidae				
5	*Alopias vulpinus*	Oceanic	Y	226–400	D
	Cetorhinidae				
1	*Cetorhinus maximus*	Coastal-pelagic	Y	500–980	E

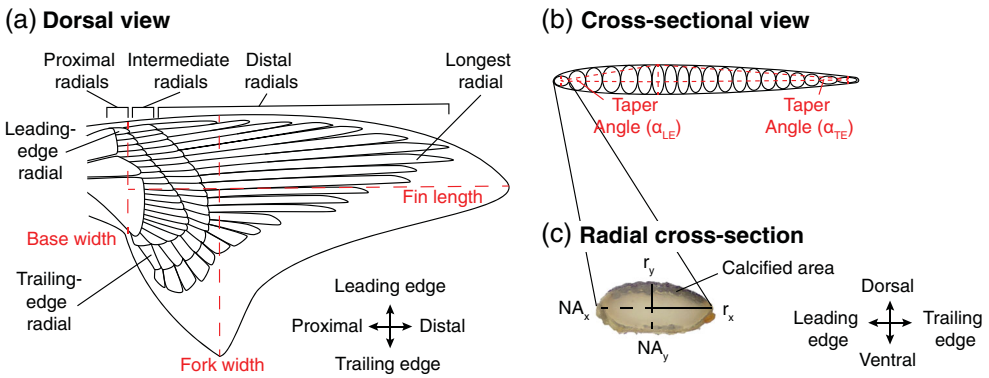

FIGURE 3 Meristics and morphometrics used to quantify pectoral fin differences among species. (a) External fin morphology was measured as the fin area, length, and width at the base and fork. Skin and connective tissue were removed to reveal the skeletal anatomy, comprised of three sets of radials that extend distally into the fin. The leading edge radial, longest radial, and trailing edge radials were further dissected to examine cross-sectional morphology (b). In general, radials were more dorsoventrally compressed on the leading and trailing edges than at the longest radial. (c) The radii along the dorsoventral (NAx; rx) and lateral (NAy; ry) neutral axes were measured to calculate the second moment of area (I) in each axis. Total and calcified areas were measured for each cross section as well

Ecomorphotype B represents smaller-bodied, non-migratory species with average size at maturity between 85 and 120 cm, and includes the Atlantic sharpnose shark, blacknose shark, and bonnethead. Ecomorphotype C includes the finetooth shark, blacktip shark, sandbar shark, and scalloped hammerhead. The species in this group undergo coastal migrations, with average size at maturity ranging from 145 to 207 cm. The final group, Ecomorphotype D, represents large bodied species, maturing on average at 227–475 cm, which are highly migratory and includes the blue shark, dusky shark, silky shark, tiger shark, great hammerhead, porbeagle, shortfin mako shark, common thresher shark, and white shark.

2.2 | External morphology

Scaled images of the dorsal and ventral side of the fin were captured with a Nikon D3500 DSLR mounted and leveled perpendicular to the fin (Nikon, Tokyo, Japan). Fin area (A_f), length (L_f), and width (W_b; W_f) were measured in ImageJ (Schneider, Rasband, & Eliceiri, 2012). Fin length was measured as the perpendicular straight-line distance from the base to the distal fin tip (Figure 3a). Fin width was measured at the (a) base as the perpendicular straight-line distance from the leading edge to the posterior margin of the trailing edge lobe (W_b) and (b) fork as the perpendicular straight-line distance from the leading edge to the most posterior portion of the trailing edge lobe (W_f) (Figure 3a). Fin AR was calculated as:

$$\mathrm{AR} = \frac{{L_f}^2}{A_f} \tag{1}$$

2.3 | Geometric morphometrics of fin shape

We used geometric morphometrics to quantitatively describe and compare the pectoral fin shape of each species in our dataset. We identified five functionally homologous locations on the pectoral fin to serve as landmarks and recorded the Cartesian coordinates of these locations on each shark fin using the digital images described above with the program tps-Dig v.2.2 (Figure 4; Rohlf, 2007): (a) proximal insertion of the trailing lobe, (b) distal tip of trailing lobe, (c) inflection of the trailing edge fork, (d) distal fin tip, and (e) proximal base of leading edge. We performed a Procrustes superimposition on the landmark arrays of all specimens to remove the effects of scale, position, and rotation (i.e., nonshape variables) on the coordinate positions of our variables using functions in the R package "geomorph" (Adams, Collyer, Kaliontzopoulou, & Sherratt, 2016; Adams & Otarola-Castillo, 2013; R Core Team, 2017). We created species averages of the landmark arrays using the custom R script from (Buser, Burns, & Lopez, 2017).

2.4 | Skeletal morphology

Skin, connective tissue, and ceratotrichia were carefully removed to expose the pectoral fin skeleton (Figure 3a). Scaled images of the dorsal and ventral side of each fin skeleton were taken with a Nikon D3300 (Nikon, Tokyo, Japan). The number of radials (n_r), skeletal area (A_{sk}), and the length of the longest radial (L_{sk}) were measured in ImageJ (Schneider et al., 2012). The amount of skeletal support was calculated as the ratio of areas (skeletal extent area; SE_a)

$$\mathrm{SE}_a = \frac{A_{\mathrm{sk}}}{A_f} \tag{2}$$

and the ratio of the lengths (skeletal extent length; SE_l)

$$\mathrm{SE}_l = \frac{L_{\mathrm{sk}}}{L_f} \tag{3}$$

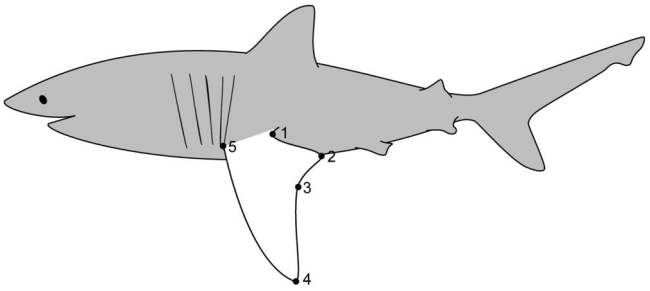

FIGURE 4 Landmarks used for shape analysis. Outline from lateral photograph of the left pectoral fin of *Carcharhinus limbatus* (fork length 67 cm, fin length 13.8 cm) used in this study. Five functionally homologous landmarks are indicated on the outline of the pectoral fin: (1) proximal insertion of the trailing lobe, (2) distal tip of trailing lobe, (3) inflection of the trailing edge fork, (4) distal fin tip, and (5) proximal base of leading edge as described in Figure 3

2.5 | Cross-sectional morphology

Cross-sectional morphology was measured for the most proximal and intermediate radial at three regions moving rostro (leading edge)-caudally (trailing edge) across the fin: the leading edge, longest, and trailing edge radial (Figure 3b). The longest radial position differed slightly among species and was most notable in the distal fin, but was the most standardized way to compare among the varied morphologies present in the study. Scaled images of the cross sections were taken using a Leica EZ4 W Stereo Microscope when small enough, and a Nikon D3300 when radial size exceeded the size of the microscope stage (Nikon, Tokyo, Japan; Leica Microsystems, Buffalo Grove, IL). The areas of calcification (A_c) and total area (A_t) were measured in ImageJ to calculate percent calcification of the radial cross section (% A_r) as

$$\%A_r = \frac{A_c}{A_t} \times 100 \tag{4}$$

Since radials are approximately elliptical in cross-sectional shape, radial shape (S_r) was characterized by calculating the second moment

of area (I) along both the x (proximo-distal) and y (dorso-ventral) neutral axes

$$I_y = \frac{\Pi r_y r_x^3}{4} \quad (5)$$

$$I_x = \frac{\Pi r_x r_y^3}{4} \quad (6)$$

(Figure 3b; Mulvany & Motta, 2013). In order to estimate the flexibility of individual skeletal elements in cross section, we measured the distribution of material (I) in the dorsoventral (x) and lateral (y) planes and radial shape (S_r) was calculated as

$$S_r = \frac{I_y}{I_x} \quad (7)$$

(Mulvany & Motta, 2013). We used I_y:I_x to describe the shape of a radial such that a value of one represents equal resistance to bending in all planes, less than one represents greater resistance to bending in the dorsoventral plane, and greater than one represents greater resistance to bending in the lateral plane (Vogel, 2003; Mulvany & Motta, 2013). Thus, the greater the I_y:I_x, the more flexible an element is in bending in the dorsoventral plane.

Whole fin cross-sectional morphology was analyzed by examining the amount of taper, or change in width, from the leading edge to the longest radial (leading edge taper, T_{LE}) and from the longest radial to the trailing edge (trailing edge taper; T_{TE}). Taper was calculated as

$$T_{LE} = \frac{D_{long} - D_{leading}}{W_s} \quad (8)$$

where D_{long} is the lateral radial diameter (2 r_x) of the longest radial, $D_{leading}$ is the lateral radial diameter along of the leading edge radial, and W_s is the segment width from the leading edge radial to the longest radial. T_{TE} was calculated using the same equation substituting leading edge for trailing edge. The taper angle (α) was calculated as:

$$\alpha = \tan^{-1}\left(\frac{T}{2}\right) \quad (9)$$

Taper angle is used to describe cross-sectional fin shape where the $T_{TE} > 0$ is indicative of tapering similar to a hydrofoil.

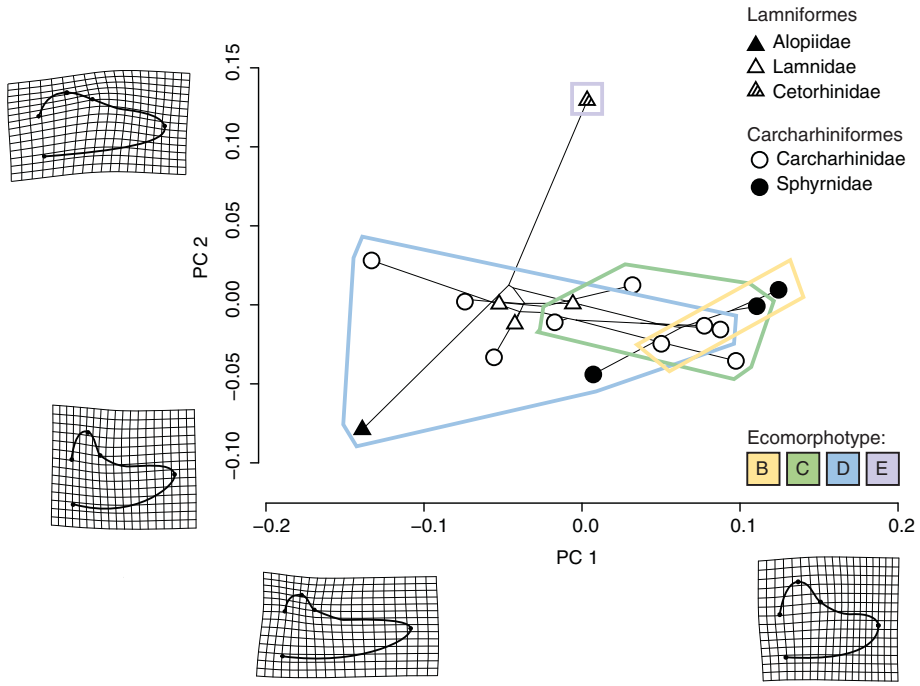

FIGURE 5 Phylomorphospace of the first two principal components of pectoral fin shape in Lamniform and Carcharhiniform sharks from Ecomorphotypes B, C, D, and E, captured using geometric morphometrics. Ecomorphotype A was represented only by Squatina, which was an outlier and whose inclusion skewed the visualization of the morphospace, so it was removed. See results section for additional details. The morphospace occupied by members of each ecomorphotype is indicated by color-coded convex hulls (outlines): yellow indicates Ecomorphotype B, green indicates C, blue D, and purple E. Phylogenetic tips represent the average morphology of each species. The symbols on tips indicate the taxonomic order to which the species belongs: triangles indicates Lamniformes, circles indicates Carcharhiniformes. The fill of the symbols represent the taxonomic family in which the species belongs: solid black triangles represent Alopiidae, solid white triangles represent Lamnidae, black and white striped triangles represent Cetorhinidae, solid white circles represent Carcharhinidae, solid black circles represent Sphyrnidae. The shape change described by each PC axis is shown at the extreme ends of each axis. Shape change is represented using an outline sketched from a photograph of a pectoral fin from *Lamna nasus*. The outline is warped here to show the shape change associated with the most extreme positive and negative values of each PC axis observed in the dataset. A thin plate spline deformation grid is overlaid to illustrate the interpolated shape change between landmark locations

2.6 | Data analysis

We used phylogenetic multivariate analysis of variance (phyMANOVA) to test for differences in average pectoral fin morphology across each of our discreet habitat guilds. We used a phylogenetic hypothesis of the relationships of all species included in this study inferred from publicly available molecular data deposited on GenBank (supplementary online material S1), which closely matches the phylogenetic hypothesis of these species published in the most current and extensive phylogenetic study of elasmobranchs (Naylor et al., 2012). We quantified pectoral fin morphology in two ways: (a) using the landmark-based dataset described above and (b) using the variables described above: skeletal extent, AR, taper, radial calcification, and radial shape. In both datasets, we calculated species averages of each trait, except for the blacknose shark, tiger shark, finetooth shark, and basking shark for which we only have one representative sample. Because of these single representatives, statistical tests were run on the species grouped by ecomorphotype or family. We acknowledge the limitations in inference this limited sample size poses at the species level and discuss findings in the context of family and ecomorphotype groups.

For the measured variables, we visually assessed normality using a quantile–quantile plots in the R statistical environment (R Core Team, 2017). For each dataset, we visualized the variance therein using a principle components analysis (PCA) and overlaid the phylogenetic relationships of the species using the phylomorphospace method of (Sidlauskas, 2008) using basic functions in R as well as functions from "geomorph" (Adams et al., 2016; Adams & Otarola-Castillo, 2013). We used functions from the R package GEIGER (Harmon et al., 2008) to perform the phyMANOVA. We examined differences among ecomorphotypes and families using one-way ANOVAs with post hoc Tukey HSD comparisons. We also examined the relationships between morphological variables using linear regressions.

3 | RESULTS

Preliminary results indicated that *Squatina* is a major outlier in the dataset, potentially skewing the results of our comparative analyses, so we removed the taxon and repeated our phylogenetic comparative analyses without it, but found no difference in outcomes. However, the presence of *Squatina* did have a considerable impact on the visualization of variance in our dataset through PCA, as the shape difference between *Squatina* and the remaining taxa dominated PC1 and made the shape differences among the remaining taxa far less appreciable. We therefore used the dataset with *Squatina* removed for showing the trends in pectoral fin shape across our dataset. There was no significant difference in pectoral fin shape across ecomorphotypes (Figure 5). While this result suggests that there is some constraint on fin shape, we do find significant differences in the internal anatomy of the fins between the ecomorphotypes. We also find significant relationships among morphological features that describe some trends across the ecomorphotype spectrum, which we discuss below.

3.1 | Geometric morphometrics and phylogenetic comparative methods

For the landmark-based dataset, the first two principal components capture approximately 62% and 17% of the observed variance in our dataset, respectively (Figure 5; Supplementary Material 2). Principal component 1 captures variation in the elongation of the leading edge of the pectoral fin, such that positive values of PC1 are associated with a relatively short leading edge and negative values are associated with a relatively long leading edge. The second principal component captures variation in the length of the trailing edge and degree of forkedness of the fin, such that high values of PC2 are associated with fins with a relatively wide base and virtually no fork, while low values of PC2 are associated with fins with a relatively narrow base and a deep fork (Figure 5).

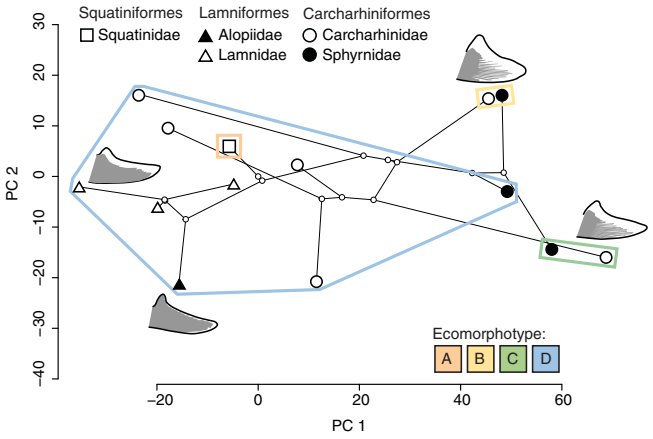

FIGURE 6 Phylomorphospace of the first two principal components of pectoral fin morphology in Lamniform and Carcharhiniform sharks from Ecomorphotypes A, B, C, and D captured using measures of gross anatomy and the internal skeleton. The morphospace occupied by members of each ecomorphotype is indicated by color-coded convex hulls (outlines): orange indicates Ecomorphotype A, yellow indicates B, green C, and blue D. Phylogenetic tips represent the average morphology of each species. The symbols on tips indicate the taxonomic order to which the species belongs: square indicates Squatiniformes, triangle indicates Lamniformes, circle indicates Carcharhiniformes. The fill of the symbols represent the taxonomic family in which the species belongs: solid white square indicates Squatinidae, solid black triangle represents Alopiidae, solid white triangle represents Lamnidae, solid white circles prepresent Carcharhinidae, and solid black circles represent Sphyrnidae. The shape and extent of calcification of the pectoral fin of each taxon with the most extreme value of each PC axis is illustrated at the location of said species in morphospace: PC1+, *Carcharhinus limbatus*; PC1−, Carcharadon carcharias; PC2+, *Sphyrna tiburo*; PC2−, *Alopias vulpinus*. For each pectoral fin outline, the extent of skeletal support is shaded in grey

For the dataset of measured variables, the first two principal components capture approximately 40% and 15% of the observed variance in our dataset, respectively (Figure 6). Species values along the first principal component are positively associated with the percent calcification of the intermediate radial of the leading edge, the percent calcification of the proximal radial along the longest radial, the percent calcification of the proximal radial along the trailing edge, and the percent calcification of the intermediate portion of the longest radial. Taken together, these variables represent how calcified the skeletal elements are at all sampled points in the fin. Species' PC2 values are positively associated with the percent area of skeletal extent (positive association) and the percent of radial support, and negatively associated with the skeletal extent of the longest radial (positive association), and percent calcification of the intermediate radial along the trailing edge (negative association; see Figure 6).

There is no statistically significant difference in the mean fin shape across the ecomorphotype groups tested herein ($p > .6$). The substantial overlap of the three groups is visually obvious in the morphospace derived from the landmark dataset (Figure 5). There is, however, a statistically significant difference in the internal anatomy of the fins between the ecomorphotype groups ($p < .008$, $R^2 = .519$). The morphospace of the first two principal components shows clear separation of Ecomorphotypes B, C, and D (Figure 6). The internal anatomy of the fins of the species making up Ecomorphotypes B and C is characterized by high values of PC1, but Ecomorphotype B is further characterized by high values of PC2, while Ecomorphotype C is characterized by low values of PC2 (Figure 6).

3.2 | Gross morphology

Fin shapes and skeletal extent vary among the species documented in this study (Figure 7). For most species, the leading edge lobe is longer than the trailing edge lobe and, it is generally more supported by the radial elements. The relative length of the leading edge lobe accounted for the majority of differences (60%) among species in the geometric morphometric analysis (PC1, Figure 5). The relative width of the fin base accounted for another 28% of the variation (PC2, Figure 5).

We found that Ecomorphotype A had the most radials compared to all other groups, among which there were no other difference (Figure 8a, $F_{5,54} = 77.26$, $p < .0001$). We hypothesized there would also be differences in AR among ecomorphotypes which was not

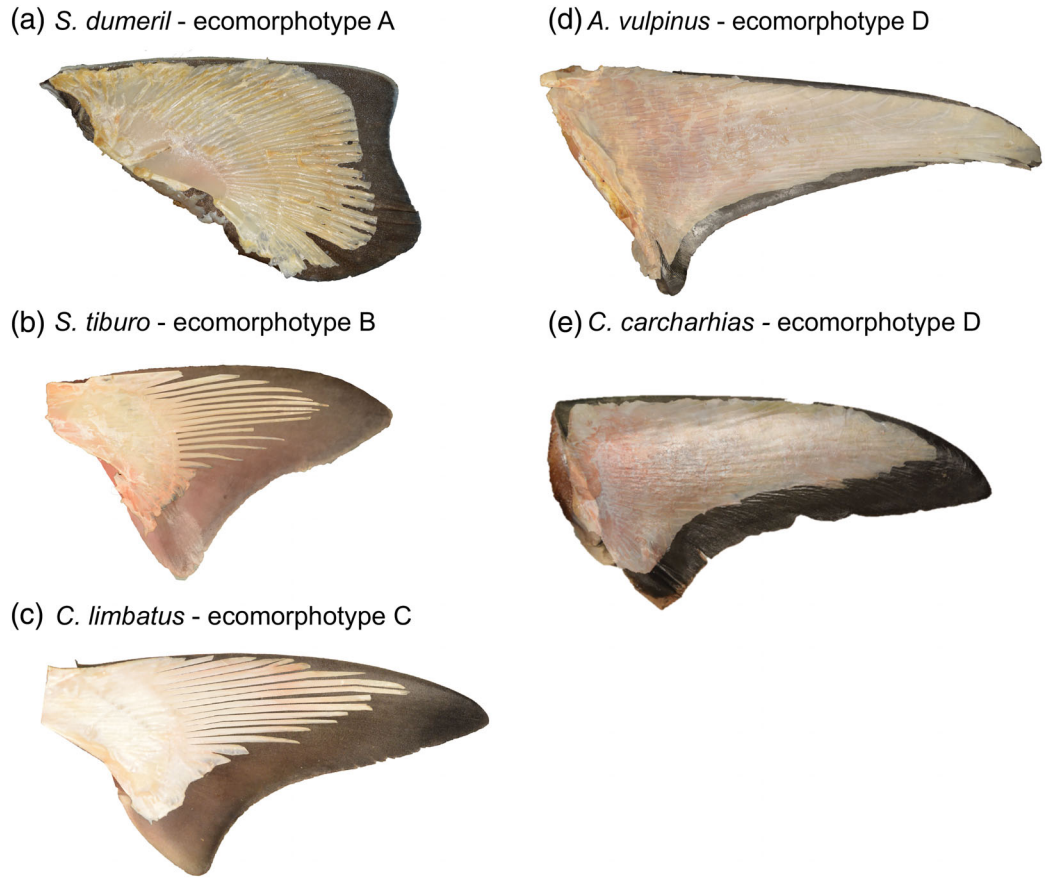

FIGURE 7 Exemplar fin overlays for five shark families demonstrating fin shape and the extent of skeletal support among families. Squatinidae (a; Ecomorphotype A) and Alopiidae (d; Ecomorphotype D) had the greatest amount of radial support, Lamnidae (e; Ecomorphotype D) was intermediate, and Sphyrnidae (b; Ecomorphotype B) and Carcharhinidae (c; Ecomorphotype C) had the least amount of radial support

supported (Figure 8b). We did find significant differences in skeletal extent among ecomorphotypes (Figure 8c, $F_{5,54}$ = 22.28, p < .0001). Ecomorphotype D had significantly more skeletal extent than Ecomorphotype B, but was not significantly different from E, C, or A. There is a gradual increase in skeletal extent from Ecomorphotype B to E, and we hypothesize that increased sample sizes may have revealed a significant trend (Figure 8c). The increase in skeletal support across the ecomorphotype spectrum from small bodied, nonmigratory species (B) to large bodied, open ocean species (D, E) supports our hypothesis. Ecomorphotype A had significantly greater skeletal support than Ecomorphotype B and was not different from all other groups (Figure 8c, p = .001).

Differences in the areas of radial support occurred at the distal fin web and trailing edge (Figure 7). For example, almost the entirety of the common thresher shark (*A. vulpinus*) fin is supported by radials; the white shark (*Carcharadon carcharias*) fin also has extensive radial support toward the distal region but the trailing edge lacks skeletal elements. In contrast, the bonnethead (*Sphyrna tiburo*) fin lacks support both in the distal end and the trailing edge (Figure 7). This species of hammerhead (bonnethead, Ecomorphotype B) is non-migratory and smaller bodied than the other representatives, the scalloped hammerhead (*S. lewini*, C) and great hammerhead (*Sphyrna mokarran* D), both had more skeletal extent. The exception to this pattern is the Atlantic angel shark (*Squatina dumeril*) fin, which is highly supported

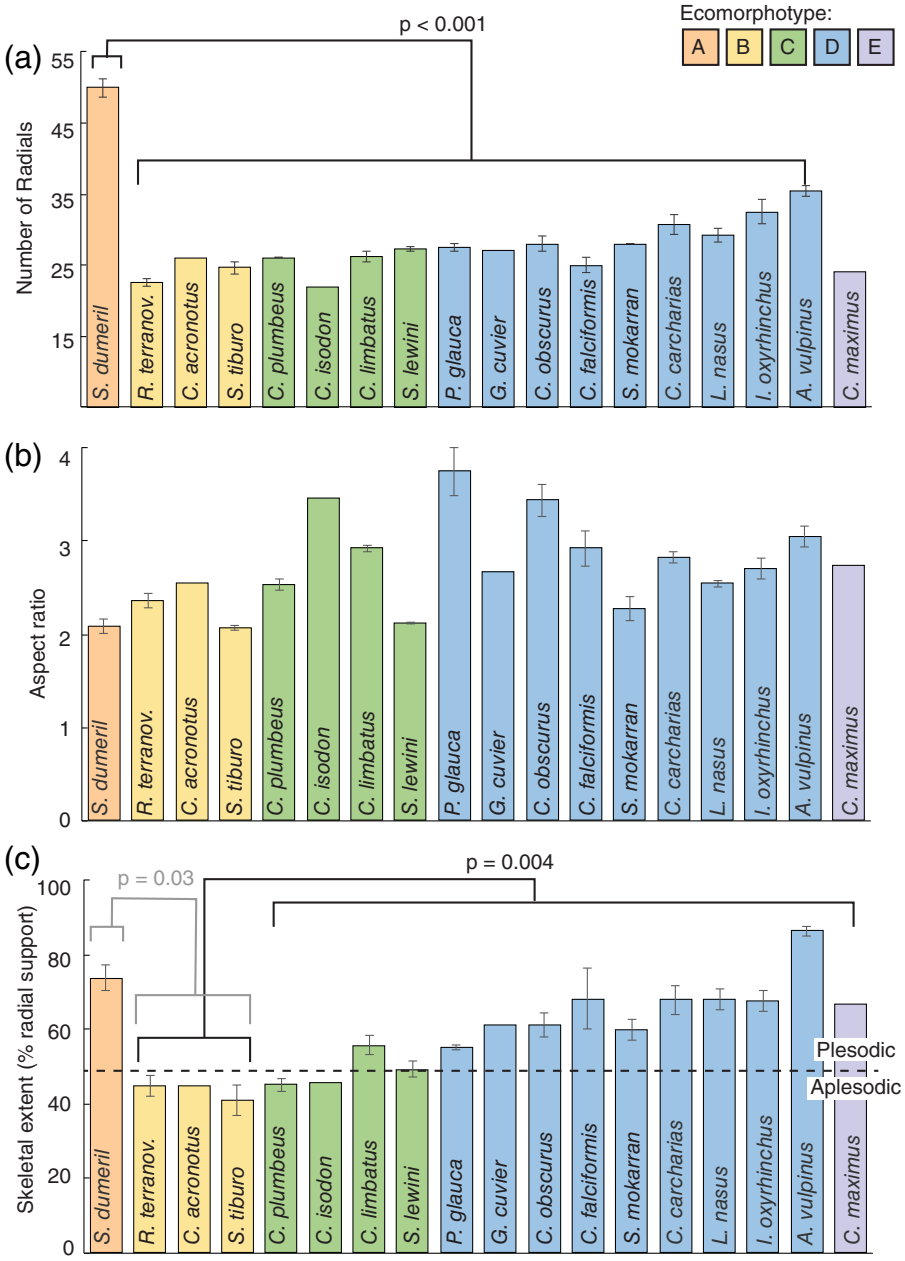

FIGURE 8 Fin classification and shape by species. Statistical differences among ecomorphotypes were tested and significance is represented with brackets and the associated p values. (a) The number of radials present in the fin was greatest for Ecomorphotype A while there were no other differences among ecomorphotypes. (b) Aspect ratio varied greatly among orders and there was no real trend among the groups. (c) Five species in Ecomorphotypes B and C, all Carcharhiniformes, had aplesodic fins. All species in Ecomorphotypes A, D, and E had plesodic fins. Ecomorphotypes A and D had significantly greater skeletal extent than Ecomorphotype B. In the observed species, skeletal extent ranged from 40 to 86%. The majority of the unsupported fin web, particularly in the plesodic fins, was along the trailing edge (see Figure 7). Error bars represent the *SEM*

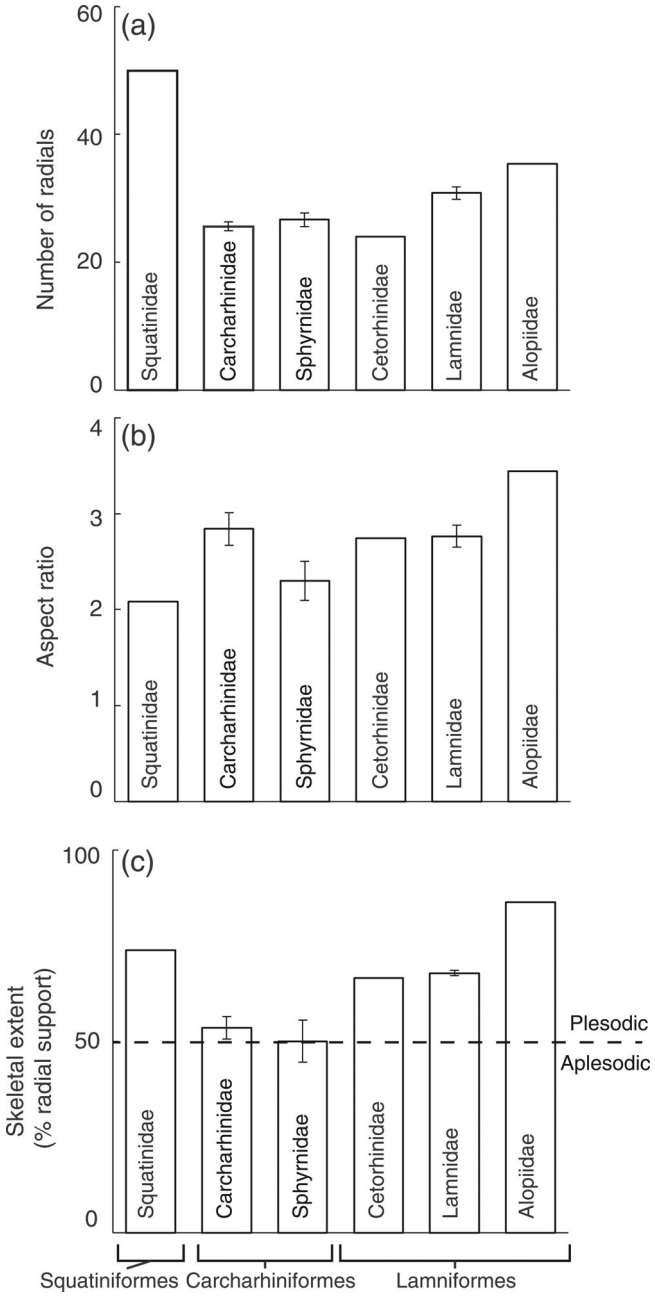

FIGURE 9 External and skeletal morphology by family and order. (a) The number of radials was substantially greatest in Squatinidae and least in Carcharhinidae, Sphyrnidae, and Cetorhinidae. Lamnidae and Alopiidae were intermediate. (b) Alopiidae had on average the greatest aspect ratio and (c) skeletal support. On average, all families observed in this study can broadly be classified as having plesodic fins, despite the differences observed by species (see Figure 8) Error bars represent the *SEM*

throughout the proximal fin area, while only the distal edge of the fin is unsupported.

The number of radials varied among species examined in this study: 22–28 (Carcharhinidae), 24–28 (Sphyrnidae), 24 (Cetorhinidae), 29–33 (Lamnidae), 35 (Alopiidae), and was greatest in Squatinidae (50) (Figure 9a). AR of pectoral fins ranged from 2.1 (Squantinidae) to 3.5 (Alopiidae) (Figure 9b).

3.3 | Cross-sectional morphology

To describe cross-sectional fin morphology, we measured the shape and calcification of the proximal and intermediate radial at three points throughout the fin: leading edge, longest radial, and the trailing edge (Figure 3b). We lacked cross-sectional data for the one representative of Ecomorphotype E. For all other ecomorphotypes, the trailing edge radial was the most dorsoventrally compressed, followed by the leading edge radial, while the longest radial was the least dorsoventrally compressed (Figure 10a). Only Ecomorphotypes A and D had radials that were more laterally compressed than a perfect circle (Figure 10a). The longest radial for Ecomorphotype D was significantly less dorsoventrally compressed than Ecomorphotypes B and C, which was the only difference among all radials (Figure 10a).

There were no significant differences between ecomorphotypes for calcification of any radials (Figure 10b). In general, Ecomorphotypes A and D had the least among of radial calcification, while calcification was greater in B and C.

For all ecomorphotypes except (C), trailing edge taper was greater than leading edge taper (Figure 10c). Ecomorphotype B and D had substantially greater trailing edge than leading edge taper (2×, 2.5×, respectively), while trailing edge taper was less than leading edge taper Ecomorphotype C (0.5×). Trailing edge taper was significantly greater for Ecomorphotype D in comparison to Ecomorphotypes B and C ($p < .05$).

3.4 | Relationships among morphological variables

To describe variations in pectoral fin morphology that have been previously overlooked, we examined the relationships between external and cross-sectional shape to skeletal support, which is historically used to classify fin shape and thus, phylogeny. Considering all species, there was no relationship between AR and skeletal extent (Figure 11a; $p = .0641$, $R^2 = .1981$).

Skeletal extent was positively related to the number of radials (Figure 11b; $p = .0051$, $R^2 = .3965$). Trailing taper angle was positively correlated with skeletal extent (Figure 11c; $p = .0017$, $R^2 = .5453$, but there were no significant relationships between the cross-sectional morphology (shape and calcification) of the trailing edge radials and skeletal extent, thus only comparisons with the leading edge and longest radial are displayed. Radial calcification was negatively related to skeletal extent along both the leading edge ($p = .0133$, $R^2 = .4120$) and longest radial ($p = .0311$, $R^2 = 03101$; Figure 11d). Similarly, radial shape was negatively related to skeletal extent, but only along the longest radial (Figure 11e; $p = .0031$, $R^2 = .5033$). Among all species, the longest radial was significantly more calcified ($F_{1,90} = 3.9469$; $p = .0420$) and the least dorsoventrally compressed than the leading edge radial ($F_{1,90} = 3.9469$; $p < .0001$).

We further analyzed species within Carcharhiniformes which was the only order to encompass multiple ecomorphotypes (B, C, and D) and the number of species represented provides a broader insight to morphological variation within an order (Table 1). There was a significant relationship between skeletal support and AR and trailing edge

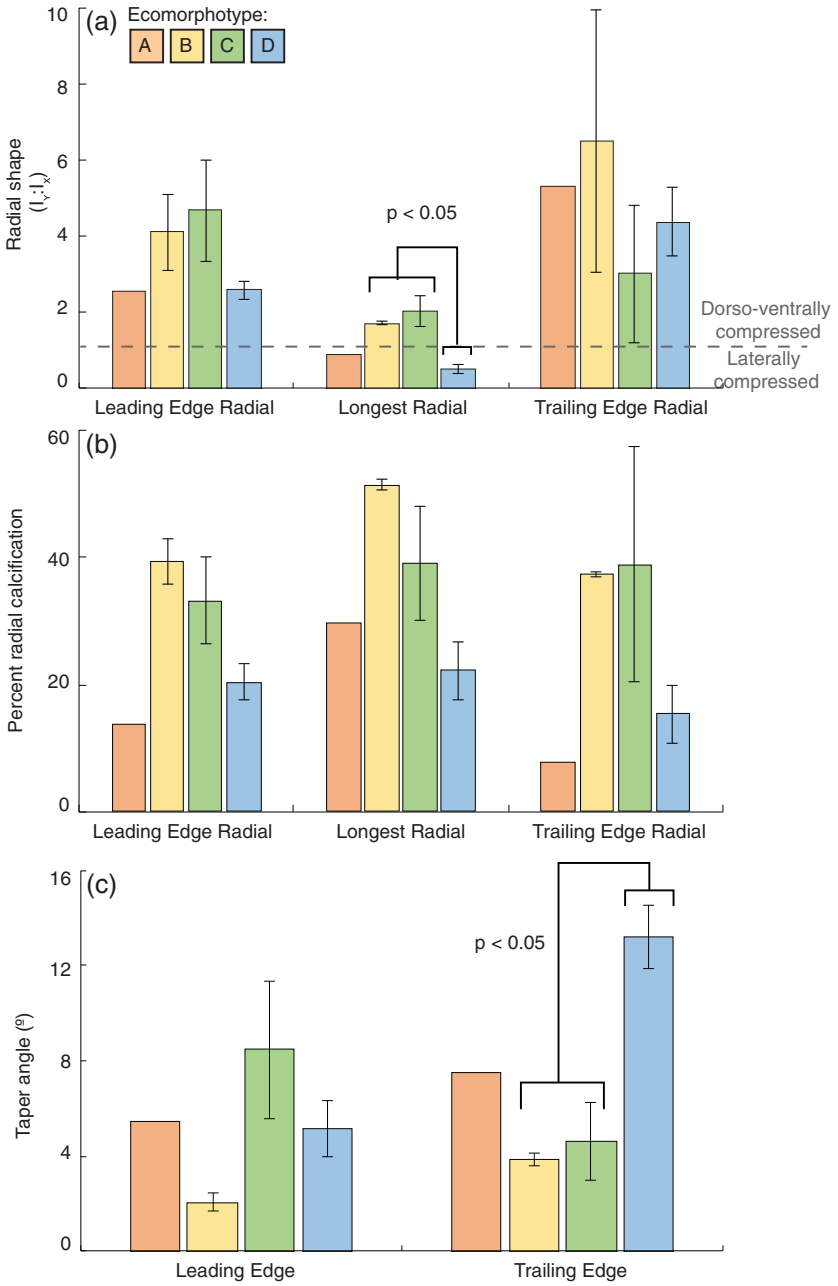

FIGURE 10 Cross-sectional morphology of the fin and radials. (a) For Ecomorphotypes B and C, both the leading and trailing edge radials were substantially more dorsoventrally compressed than the longest proximal radial. In Ecomorphotypes A and D was the longest radial laterally compressed. (b) The amount of calcification was highly varied among radials and ecomorphotypes, but in general, Ecomorphotype D had less radial calcification than other groups. (c) For all ecomorphotypes except C, taper angle was greater along the trailing edge. When considering the means of all species, trailing edge taper angle was significantly greater than leading edge taper angle by a factor of two (p = .0032)

taper within this order (Figure 12; p = .0201, R^2 = .4325; p = .0061, R^2 = .6307).

4 | DISCUSSION

We described a suite of morphological variables demonstrating that skeletal extent alone is not a comprehensive diagnostic of fin morphology. While we found significant differences in the internal anatomy of the pectoral fin across the ecomorphotypes considered in this study, we did not find significant differences in the overall shape of the fin. This suggests that, though the fins are superficially similar, they may be adapted for different uses in each of the environments, possibly with historical, phylogenetic constraints of fin shape in sharks. In further analyses without phylogenetic consideration, we also found significant differences in skeletal anatomy among ecomorphotypes and we discuss the implications of these contradictory results below.

4.1 | Geometric morphometrics and phylogenetic comparative methods

An analysis of fin shape using geometric morphometrics reveals that the two greatest axes of variation are the leading edge shape (62% of the observed variance in the data set) and trailing edge shape

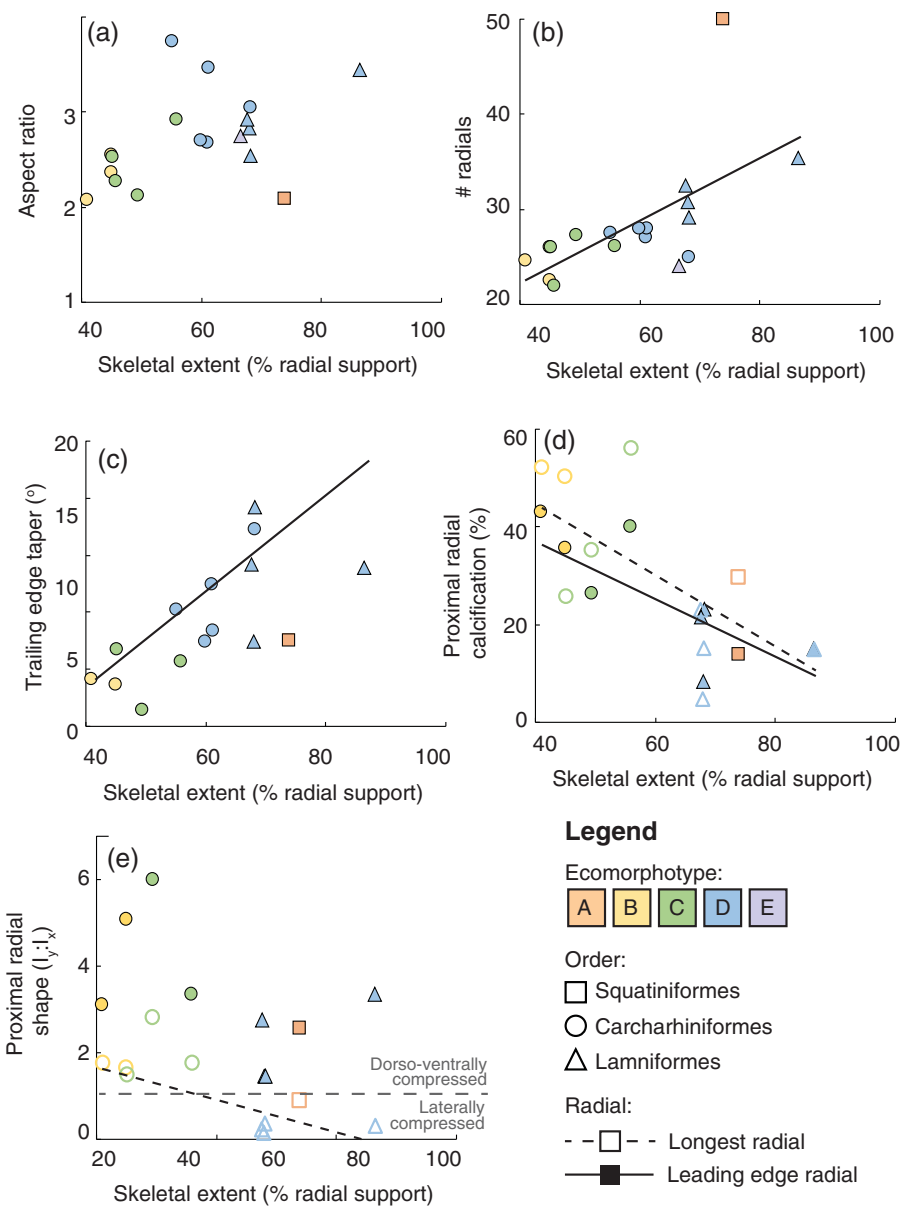

FIGURE 11 Relationship between skeletal extent and cross-sectional morphology. (a) There was no relationship between skeletal support and aspect ratio. (b) Radial support was positively related to the number of radials (p = .0051, R^2 = .3965). (e) Trailing edge taper is positively correlated with skeletal extent (p = .0017; R^2 = .5453). (d) Calcification of the proximal radial was negatively correlated to skeletal extent for both leading edge and proximal radials (p = .0133; R^2 = .4120; p = .0031; R^2 = .3101, respectively). The proximal longest radial was significantly more calcified than the leading edge radial ($F(1,90)$ = 3.9469; p = .0420). (e) Proximal radial shape was also negatively correlated with skeletal extent, but only along the longest radial (p = .0031; R^2 = .5033). Further, the proximal leading edge radial was significantly more dorsoventrally compressed than the longest radial ($F(1,90)$ = 3.9469; p < .0001)

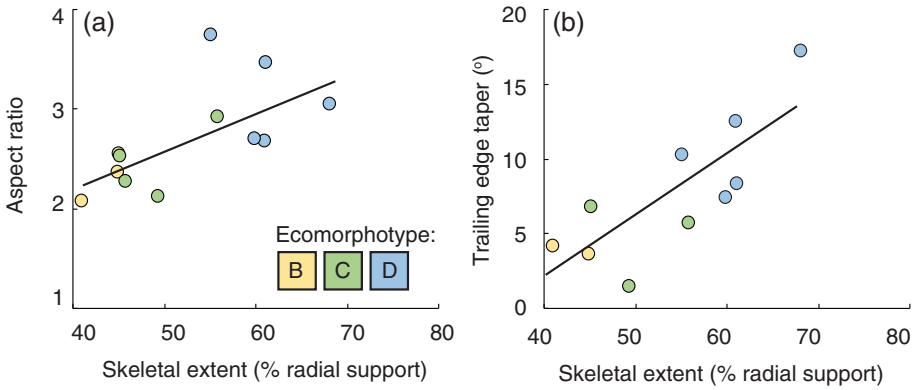

FIGURE 12 Relationship between skeletal extent and morphology in order Carcharhiniformes, separated by ecomorphotype. Both aspect ratio (a) and trailing edge taper (b) were positively related to skeletal extent (p = .0201, R^2 = .4325; p = .0061, R^2 = .6307)

considering the curvature of the fork (17%; Figure 5). Lamniform species tend to have long pectoral fins with deep forks, while Carcharhiniform species are much more variable in their pectoral fin shape (Figure 5). We also examined linear fin measurements in phylogenetic context (Figure 6). Lamniformes and Carcharhiniformes appear to separate along PC1, with Lamniformes all tending to have a high

extent of skeletal support in the pectoral fins, while there is much more variability within Carcharhiniformes. For all species, the leading edge is well supported by radials, likely making this region stiff. This may be advantageous for force generation, especially considering the hydrofoil cross-sectional shape of the fin (Figure 10a). The major differences in skeletal support appear to occur at the trailing edge (Figure 7). The Lamniform species have skeletons that support the majority of the fin web, including the trailing edge, while Carcharhiniform species have more variation in skeletal extent occurring at the distal fin tip and trailing edge (Figures 7 and 8b). Flexibility at the distal fin tip and trailing edge may allow for greater changes in fin conformational shape, and thus, a finer degree of control over small changes in pitch (Wilga & Lauder, 2000, 2001).

Skeletal extent, as well as calcification of skeletal elements, accounted for significant variation among ecomorphotypes (Figure 6). Considering these metrics together, we propose that there may be a prioritization of material distribution. For Ecomorphotype D species, it may be more beneficial to support the entire fin web with less calcified skeletal support, resulting in a larger degree of taper throughout the fin and generating a characteristic foil shape (Figure 10c). On the other end of the spectrum, Ecomorphotype B species may rely on greater amounts of calcification in their less extensive skeleton, resulting in a less tapered fin that is still able to produce necessary forces for maneuvering. Less extensive skeleton in the trailing edge may also aid in maneuverability since the unsupported portion of fin is more flexible and may be able to move independently, hinging at the edge of the supported region. In essence, the trailing edge could act as a spoiler, contributing to destabilizing forces during maneuvering (Figures 6 and 7).

Phylogenetic bias is accounted for using the phyMANOVA, but suggests a separation of species by ecomorphotype. Although there were no significant differences in fin shape among ecomorphotypes, other morphological features observed in this study may confer seemingly adaptive advantages to life in oceanic (Ecomorphotype D) versus inshore (Ecomorphotype B) habitats and we discuss these below.

4.2 | Gross morphology

We compared AR among ecomorphotypes and families as a proxy for hydrodynamic efficiency, and hypothesized that AR would also be greatest in open ocean species (Ecomorphotypes D and E). We found no differences in AR among ecomorphotypes (Figure 8b), but there were significant differences when compared among families (Figure 9b). In combination with results from the phylogenetic analyses, this suggests that there may be some phylogenetic constraint on fin shape (Figures 5, 6, and 9). Squantinidae (Ecomorphotype A) had significantly lesser AR fins in comparison to Alopiidae (Ecomorphotype D) which represent opposite ends of our ecomorphotype spectrum, but there was no clear trend among ecomorphotypes (Figures 8b and 9b). The species documented in this study fall within a small AR range from 1.8 to 3.5, which is comparable to AR described previously for a number of actinopterygian caudal and pectoral fins (Binning & Fulton, 2011; Fulton et al., 2005; Sambilay Jr, 1990). Lesser AR fins are typically characteristic of species that use drag-based swimming, such as pectoral fin paddling, while greater AR fins may be indicative of species using lift-based swimming (Fulton et al., 2005; Vogel, 1994; Wainwright et al., 2002). In labrid fishes, AR is related to fin attachment to the body: fins with greater AR attach at a shallower angle allowing greater motion in the dorsoventral axis, suggesting lift-based locomotion (Wainwright et al., 2002). Although sharks rely primarily on body-caudal fin swimming, differences in fin AR and attachment to the body may indicate a difference between drag-based and lift-based thrust production, but in maneuvering rather than straight swimming. Further analyses, similar to the comprehensive studies of fin AR and swimming performance in actinopterygian fishes, would greatly benefit our understanding of the relationship between shark fin shape, locomotor performance, and habitat use (Fulton et al., 2005; Fulton & Bellwood, 2004; Lauder & Drucker, 2004; Wainwright et al., 2002; Walker & Westneat, 2002).

The analysis of shark fin morphology and function often centers on a dichotomous classification into aplesodic or plesodic fins, referring to the percentage of the fin supported by the cartilaginous skeletal elements (Maia et al., 2012; Sakai, 2011). In this study, we demonstrate that skeletal support is more appropriately described as a continuum rather than the binary classification that is historically relied upon. When considering the traditional categorization of skeletal extent, we find a range from aplesodic to plesodic (Figure 8c). Aplesodic fins were found in Ecomorphotypes B and C, whiles Groups D, E, and A were comprised of plesodic fins. We hypothesized that there would be a spectrum in skeletal extent from benthic species (Ecomorphotype A) to oceanic species (Ecomorphotypes D and E). We did find significant differences in skeletal extent between Ecomorphotypes B and D, with a qualitative increase across the spectrum (Figure 8c). The exception to this trend was Ecomorphotype A, in which the only representative is the Atlantic angel shark. This species has previously been classified as plesodic, and other groups that would fit into Ecomorphotype A (such as species from Squaliformes or Heterodontiformes) have been considered aplesodic (Figure 2). This study was limited by access to species in Ecomorphotype A and future studies would benefit from increasing sample sizes in this group.

Of interest, all families represented in this study are previously classified as plesodic, exemplifying one issue in using these discrete categories (Figures 2 and 9c). Since we document differences in skeletal extent within families, we suggest that fin morphology should be evaluated at the species level. When considered at the family level, variation is low but the resolution at the delineation between aplesodic and plesodic is lost. Perhaps even more precise would be to refer to skeletal extent continuously, rather than as binary categories. The hypothesis that aplesodic fin support is the ancestral condition from which plesodic fins arose may lend too much credence to the idea that these are two discrete states (Compagno, Ebert, & Smale, 1989). Our data demonstrate that differences in fin shape and skeletal anatomy are explained by phylogenetic relationships, thus considering skeletal extent as a continuous variable rather than a categorical condition may be more applicable (Figures 5 and 6).

The differences in internal anatomy that we found across ecomorphotypes may reflect differences in function. More skeletal support is hypothesized to increase overall fin stiffness, since the anatomical components that make up the nonskeletonized portion of the fin are flexible ceratotrichia, skin, and connective tissue (Maia et al., 2012; Sakai, 2011; Figure 1). Ecomorphotypes A, D, and E all have extensive skeletal support, and would be hypothesized to have stiffer fins, that serve different functions based on the habitats of these groups. Ecomorphotype D comprises larger bodied, open ocean species, of which Lamnidae and Alopiidae could be considered high performance predators (Compagno, 1984). Stiffer fins in this environment likely minimize drag and generate more lift, thereby increasing swimming efficiency. Squatiniformes (Ecomorphotype A), on the other hand, are benthic sharks that commonly interact with the substrate (Compagno, 1984). In this environment, fins with more extensive skeletal support may be beneficial for weight bearing behaviors such as burrowing, resting, or punting from the substrate (Compagno, 1984).

When grouped by family, there was little variation in gross morphological characteristics, particularly among Lamniformes (Figure 9). The Lamniformes species sampled here have similar body types, habitat use, and locomotor style, excluding the basking shark (*C. maximus*), which tends to be a slow swimming, filter feeding species (Compagno, 1984). Of the orders examined, Carcharhiniformes had the most variation in skeletal extent, ranging from 40 to 70% (Figure 8c). This was the only order with variability in ecomorphotype, making it good candidate for comparative analyses among species (Table 1). When separated, there was a significant relationship between skeletal extent and AR in this order, which was not true for the whole dataset (Figures 11 and 12). Additionally, there was a clearer trend across the ecomorphotype spectrum in AR, skeletal extent, and trailing edge taper (Figure 12). We hypothesize that this difference in fin morphology exemplifies a functional tradeoff between fin flexibility and hydrodynamic efficiency. Larger bodied, migratory species (Ecomorphotype D) may benefit more from hydrodynamically efficient body design for sustained cruising, but smaller bodied species that are reef associated (Ecomorphotype B) may use flexible fins for maneuvering in more architecturally complex environments (Table 1; Thomson & Simanek, 1977). This hypothesis is further supported by the inverse relationship between skeletal extent and the amount of pectoral girdle musculature: more muscle is need for a finer degree of control over flexible fins (Maia et al., 2012).

4.3 | Cross-sectional morphology

The extent of skeletal support in a fin gives some insight into its mechanical behavior, but the distribution of material and calcification within the radials may also affect overall stiffness (Mulvany & Motta, 2013; Vogel, 2003). For all families, the longest radial was the least dorsoventrally compressed, causing taper at both the leading and trailing edge (Figure 10). This gives the fin a characteristic foil shape, with greater thickness in the middle and tapering at the edges. Only Ecomorphotypes A and D had radials that were laterally compressed (I_y:I_x < 1), suggesting that these fins may resist bending in the dorsoventral plane better than the other families. Ecomorphotype D is comprised of larger bodied, oceanic sharks for whom stiff, lift producing fins would maximize lift to drag for more efficient swimming (Table 1). Further, among all species we found a significant relationship between radial shape and skeletal extent, demonstrating that fins with greater skeletal support also have radials that resist dorsoventral bending, increasing overall stiffness (Figure 11e). Contrary to our hypothesis, Ecomorphotype D had the least amount of radial calcification, and there was an inverse relationship between skeletal extent and radial calcification (Figures 10b and 11d). We hypothesize that radials in these families are shaped to resist bending and have extensive skeletal support, and the costly addition of calcification is unnecessary.

The shape of radials along the leading edge, middle, and trailing edge of all families examined in this study demonstrate a characteristic foil shape as has been hypothesized throughout the literature (Alexander, 1965; Ferry & Lauder, 1996; Harris, 1936; Maia et al., 2012). In general, foils induce less drag at high speeds if the thickness is low, making tapering an effective shape strategy to maximize lift to drag (Vogel, 1994; Webb, 1975; Weber et al., 2009, 2014). We documented trailing edge taper for all groups, with Ecomorphotype D demonstrating the most (Figure 10c). Shark pectoral fins are shown to produce lift, either during steady swimming or vertical rising, making cross-sectional hydrofoil an efficient design (Fish & Shannahan, 2000; Harris, 1936; Wilga & Lauder, 2000). We hypothesize that exaggerated taper in Ecomorphotype D may be indicative of increased lift generating potential. Further, we found a positive relationship between skeletal support and trailing edge taper, suggesting that fins with greater skeletal support, mostly Ecomorphotype D, maximize lift to drag ratios, thereby increasing hydrodynamic efficiency (Figure 11c).

5 | CONCLUSION

We found that shark pectoral fin internal anatomy significantly differs across ecomorphotypes among the 18 species examined in this study, but that the shape of the fins does not. This suggests that there may be functional differentiation and specialization of the fins, perhaps in the face of evolutionary constraint fin shapes. Here, we describe a spectrum in both gross and cross-sectional morphology that may confer functional advantages in different habitats. Taken together, these relationships between gross and cross-sectional morphology support our hypothesis that sharks from different ecomorphotypes have differing fin anatomy. At one end of the continuum, species in Ecomorphotype D appear to have fins designed to maximize hydroxamic efficiency: greater AR and skeletal extent, more radials which are laterally compressed, and a high degree of taper. At the other end, species in Ecomorphotype B have fins that may be better designed for complex fin movements: lesser AR and skeletal extent, dorsoventrally compressed radials, and an unsupported trailing edge. Within Carcharhiniformes, we observe a significant relationship among these variables, consistent with the above patterns. Squatina, the one benthic (Ecomorphotype A) representative in this study,

contradicted this hypothesis and we predict that a broader range of sampling may reveal a different trend. Further consideration of more species from a greater diversity of ecomorphotypes and families would greatly enhance our understanding of shark ecomorphology.

ACKNOWLEDGMENTS

The authors extend their sincerest thanks to L. Natanson, D. Adams, S. Kajiura, P. Motta, M. Bowers, K. Viducic, and K. James for aid in collection of pectoral fins. The authors also thank W. Lopez and C. Testagrose who conducted much of the initial dissections and imagery analyses. Two anonymous reviewers significantly improved the scope of this manuscript. This work was funded Florida Atlantic University start-up funds to M. E. P, Florida Atlantic University Newell Doctoral Fellowship, and Delores. A. Auzenne Fellowship to S. L. H. A grant from the United States National Science Foundation (IOS-1941713) to MEP contributed, in part, to this work.

AUTHOR CONTRIBUTIONS

Sarah L. Hoffmann: Conceptualization; data curation; formal analysis; funding acquisition; investigation; methodology; project administration; resources; software; supervision; validation; visualization; writing-original draft; writing-review and editing. **Thaddaeus J. Buser:** Formal analysis; methodology; software; validation; visualization; writing-original draft; writing-review and editing. **Marianne E. Porter:** Conceptualization; funding acquisition; project administration; resources; supervision; writing-original draft; writing-review and editing.

PEER REVIEW

The peer review history for this article is available at https://publons.com/publon/10.1002/jmor.21269.

DATA AVAILABILITY STATEMENT

The data that support the findings of this study are openly available in GitHub at https://github.com/hoffmannsarahlouise/FinMorph, DOI: 10.5281/zenodo.3981273.

ORCID

Sarah L. Hoffmann https://orcid.org/0000-0003-3376-0121

REFERENCES

Adams, C., Collyer, M., Kaliontzopoulou, A., and Sherratt, E. (2016). *Geomorph: Software for Geometric Morphometric Analyses. R Package Version 3.0.5*.

Adams, D. C., & Otarola-Castillo, E. (2013). Geomorph: An R package for the collection and analysis of geometrics morphometric shape data. *Methods in Ecology and Evolution*, *4*(4), 393–399.

Alexander, R. M. (1965). The lift produced by the heterocercal tails of selachii. *The Journal of Experimental Biology*, *43*(1), 131–138.

Bendix-Almgreen, S. E. (1975). *The paired fins and shoulder girdle in Cladoselache, their morphology and phyletic significance*. France: Colloques Internationaux Centre National de la Recherche Scientifique.

Binning, S. A., & Fulton, C. J. (2011). Non-lethal measurement of pectoral fin aspect ration in coral reef fishes. *Journal of Fish Biology*, *79*(3), 812–818.

Blake, R. W. (2004). Fish functional design and swimming performance. *Journal of Fish Biology*, *65*(5), 1193–1222.

Buser, T. J., Burns, M. D., & Lopez, J. A. (2017). Littorally adaptive? Testing the link between habitat, morphology, and reproduction in the intertidal sculpin subfamily Oligocottinae (Pisces: Cottoidea). *PeerJ*, *5*, e3634.

Compagno, L. J. V. (1973). Interrelationships of living elasmobranchs. In P. H. Greenwood, R. S. Miles, & C. Patterson (Eds.), *Interrelationships of fishes*. London, England: Academic Press.

Compagno, L. J. V. (1977). Phyletic relationships of living sharks and rays. *American Zoologist*, *17*, 303–322.

Compagno, L. J. V. (1984). FAO species catalogue. In *Sharks of the world* (Vol. 4). Rome: Food and Agricultural Organization of the United Nations.

Compagno, L. J. V. (1988). *Sharks of the order Carcharhiniformes*. Princeton, NJ: Princeton University Press.

Compagno, L. J. V., Ebert, D. A., & Smale, M. J. (1989). *Guide to the sharks and rays of southern Africa*. London, England: New Holland Publishers.

Compango, L. J. V. (1990). Relationships of the megamouth shark, *Megachasma pelagios* (Lamniformes: Megachasmidae), with comments on its feeding habits. In: H. L. Pratt Jr, S. H. Gruber, & T. Taniuchi. (Eds.), Advances in the biology, ecology, systematics, and the status of the fisheries. NOAA Technical Report NMFS 90. U.S. Department of Commerce, Washington, DC, 357–379.

Crawford, C. H. (2014). *Skeletal anatomy in the chondrichthyan tree of life* (Vol. 2014). Charleston, SC: College of Charleston.

Daniel, J. F. (1922). *The elasmobranch fishes*. Berkeley, California: University of California Press.

Ferry, L., & Lauder, G. V. (1996). Heterocercal tail function in leopard sharks: A three-dimensional kinematics analysis for two models. *The Journal of Experimental Biology*, *199*(10), 2253–2268.

Fish, F. E., & Lauder, G. V. (2017). Control surfaces of aquatic vertebrates: Active and passive design and function. *The Journal of Experimental Biology*, *220*, 4351–4363.

Fish, F. E., & Shannahan, L. D. (2000). The role of the pectoral fins in body trim of sharks. *Journal of Fish Biology*, *56*, 1062–1073.

Fulton, C. J., Bellwood, D. R., & Wainwright, P. C. (2005). Wave energy and swimming performance shape coral reef fish assemblages. *Proceedings of the Royal Society B*, *272*(1565), 827–832.

Fulton, C. J., & Bellwood, D. R. (2004). Wave exposure, swimming performance, and the structure of tropical and temperate reef fish assemblages. *Marine Biology*, *144*(3), 429–437.

Harris, J. E. (1936). The role of fins in the equilibrium of swimming fish. I. Wind-tunnel tests on a model of *Mustelus canis* (Mitchill). *The Journal of Experimental Biology*, *13*, 474–493.

Harmon, L., Weir, J., Brock, C., Glor, R., Challenger, W., & Hunt, G. (2008). Geiger: Analysis of Evolutionary Diversification. *R package version 1.3-1*.

[dataset] Hoffman, S. L., Buser, T. J., & Porter, M. E; The comparative morphology of shark pectoral fins. Retrieved from github.com/hoffmannsarahlouise/FinMorph; https://doi.org/10.5281/zenodo.3981273

Lauder, G. V., & Drucker, E. G. (2004). Morphology and experimental hydrodynamics of fish fin control surfaces. *IEEE Journal of Oceanic Engineering*, *29*(3), 556–571.

Liem, K. F., & Summers, A. P. (1999). Muscular system. In W. C. Hamlett (Ed.), *Sharks, skates, and rays: The biology of elasmobranch fishes* (pp. 93–114). Baltimore, MD: The John Hopkins University Press.

Lucas, K. N., Lauder, G. V., & Tytell, E. D. (2020). The fish body functions as an airfoil: Surface pressures generate thrust during carangiform locomotion. *bioRxiv*, *2020*.

Maia, A. M. R., Wilga, C. A. D., & Lauder, G. V. (2012). Biomechanics of locomotion in sharks, rays, and chimeras. In *Biology of sharks and their relatives* (2nd ed., pp. 125–151). Boca Raton, FL: CRC Press.

Maisey, J. G. (1984). Higher elasmobranch phylogeny and biostratigraphy. *Zoological Journal of the Linnean Society*, *82*, 33–52.

Marinelli, W., & Strenger, A. (1959). Superklasse: Gnathostomata. (Kiefermäuler). Klasse: Chondrichthyes. (Knorpelfische). In *Vergleichende Anatomie und Morphologie der Wirbeltiere. II*. Berlin Heidelberg New York: Springer-Verlag.

Mulvany, S., & Motta, P. J. (2013). The morphology of the cephalic lobes and anterior pectoral fins in six species of batoids. *Journal of Morphology*, *274*, 1070–1083.

Naylor, G. J. P., Caira, J. N., Jensen, K. J., Rosana, K. A. M., Straube, N. S., & Lakner, C. (2012). Elasmobranch phylogeny: A mitochondrial estimate based on 595 species. In *The biology of sharks and their relatives* (pp. 31–56). Boca Raton, FL: CRC Press.

R Core Team. (2017). *R: A language and environment for statistical computing*. Vienna, Austria. Retrieved from http://www.R-projectorg/: R Foundation for Statistical Computing.

Rohlf, F. J. (2007). *TPS relative warps v1.45*. Stony Brook, NY: Department of Ecology and Evolution, State University of New York at Stony Brook.

Sakai, S. A. (2011). *Morphology, ecology and function in elasmobranchs: Comparative analysis of pectoral fins*. Providence, RI: University of Rhode Island.

Sambilay, V. C., Jr. (1990). Interrelationships between swimming speed, caudal fin aspect ratio and body length of fishes. *Fishbyte*, *8*(3), 16–20.

Schneider, C. A., Rasband, W. S., & Eliceiri, K. W. (2012). NIH image to ImageJ: 25 years of image analysis. *Nature Methods*, *9*(7), 671–675.

Shirai, S. (1996). Phylogenetic interrelationships of neoselachians (Chondrichthyes: Euselachii). In M. Stiassy, L. Parenti, & G. D. Johnson (Eds.), *Interrelationship of fishes* (pp. 9–34). London, UK: Academic Press.

Sidaulaskas, B. (2008). Continuous and arrested morphological diversification in sister clades of characiform fishes: A phylomorphospace approach. *Evolution*, *62*(12), 3135–3156.

Thomson, K. S., & Simanek, D. E. (1977). Body form and locomotion in sharks. *Integrative and Comparative Biology*, *17*, 343–354.

Vogel, S. (1994). *Life in moving fluids*. Princeton, NJ: Princeton University Press.

Vogel, S. (2003). Simple Structures: Beams, columns, and shells. *Comparative biomechanics: life's physical world*, (pp.363–388). Princeton, NJ: Princeton University Press.

Velez-Zuazo, X., & Agnarsson, I. (2011). Shark tales: a molecular species-level phylogeny of sharks (Selachimorpha, Chondrichthyes). *Molecular phylogenetics and evolution*, *58*(2), 207–217.

Wainwright, P. C., Bellwood, D. R., & Westneat, M. W. (2002). Ecomorphology of locomotion in labrid fishes. *Environmental Biology of Fishes*, *65*(1), 47–62.

Walker, J. A., & Westneat, M. W. (2002). Performance limits of labriform propulsion and correlates with fin shape and motion. *The Journal of Experimental Biology*, *205*(2), 177–187.

Webb, P. W. (1975). Hydrodynamics and energetics of fish propulsion. *Bulletin—Fisheries Research Board of Canada*, *190*, 158.

Weber, P. W., Howe, L. E., Murray, M. M., Reidenberg, J. S., & Fish, F. E. (2014). Hydrodynamic performance of the flippers of large-bodied cetaceans in relation to locomotor ecology. *Marine Mammal Science*, *30*(2), 413–432.

Weber, P. W., Howle, L. E., Murray, M. M., & Fish, F. E. (2009). Lift and drag performance of odontocete cetacean flippers. *The Journal of Experimental Biology*, *212*(14), 2149–2158.

Wilga, C. D., & Lauder, G. V. (2000). Three-dimensional kinematics and wake structure of the pectoral fins during locomotion in leopard sharks *Triakis semifasciata*. *The Journal of Experimental Biology*, *203*(15), 2261–2278.

Wilga, C. D., & Lauder, G. V. (2001). Functional morphology of the pectoral fins in bamboo sharks, *Chiloscyllium plagiosum*: Benthic vs. pelagic station-holding. *Journal of Morphology*, *249*(3), 195–209.

Zangerl, R. (1973). *Interrelationships of early Chondrichthyans*. London, England: Academic Press.

SUPPORTING INFORMATION

Additional supporting information may be found online in the Supporting Information section at the end of this article.

How to cite this article: Hoffmann SL, Buser TJ, Porter ME. Comparative morphology of shark pectoral fins. *Journal of Morphology*. 2020;1–16. https://doi.org/10.1002/jmor.21269